EuroIntervention 2018;13:e2169-e2173 published online November 2017 ■ published online e-edition April 2018

Very late scaffold thrombosis: insights from optical coherence tomography and histopathology

Michael Joner[1]*, MD; Philipp Nicol[1], MD; Himanshu Rai[1], MSc, PhD; Heiko Richter[2], PhD; Nicolas Foin[3], MSc, PhD; Jaryl Ng[3], PhD; Javier Cuesta[4], MD; Fernando Rivero[4], MD; Rosario Serrano[4], MD; Fernando Alfonso[4], MD

1. Deutsches Herzzentrum München, Technische Universität München, Munich, Germany; 2. LLS ROWIAK LaserLabSolutions GmbH, Hanover, Germany; 3. National Heart Centre Singapore, Singapore; 4. Hospital Universitario de La Princesa, Madrid, Spain

This paper also includes supplementary data published online at: http://www.pcronline.com/eurointervention/133rd_issue/358

Introduction

A 79-year-old male patient had a 2.5×12 mm bioresorbable vascular scaffold (Absorb™ BVS; Abbott Vascular, Santa Clara, CA, USA) implanted in the setting of the RIBS VI study protocol for in-stent restenosis of a 3×9 mm bare metal stent (AVE S670; Medtronic, Minneapolis, MN, USA) in January 2015, at which time point the patient presented with stable angina and positive exercise stress test (index procedure). The Absorb BVS was implanted with predilatation at 20 atmospheres (atm) accompanied by post-dilatation with a non-compliant balloon (2.5×10 mm) at 26 atm. The patient was maintained on dual antiplatelet therapy (DAPT) with aspirin 100 mg and clopidogrel 75 mg for 12 months. In September 2015, protocol-mandated angiographic follow-up revealed very mild narrowing of the Absorb BVS, with an otherwise good angiographic result **(Moving image 1)**. In January 2016, DAPT was discontinued in accordance with the study protocol and the patient presented with very late stent thrombosis approximately one month following cessation of DAPT (13 months following index stenting).

At the time point of stent thrombosis, the patient presented in cardiogenic shock, with anterior ST-elevation myocardial infarction (CKmax 7,103 U/L), where immediate rescue PCI was performed including implantation of an intra-aortic balloon pump (IABP), thrombus aspiration using a 6 Fr aspiration catheter (Export®; Medtronic) and repeat balloon dilatation (semi-compliant 2.5×12 mm and non-compliant 3×12 mm at 26 atm). Despite extended revascularisation attempts, no/slow flow persisted with Thrombolysis In Myocardial Infarction (TIMI) 1 flow in the left anterior descending artery **(Moving image 2)**. The patient was transferred to the intensive care unit (ICU), where IABP therapy was maintained for six hours. Despite maximum ICU support including vasopressors and IABP, the patient died in refractory cardiogenic shock eight hours following admission to hospital.

Methods

Optical coherence tomography (OCT) was performed in the cath-lab according to current consensus[1,2]. Following complete autopsy,

*Corresponding author: Deutsches Herzzentrum München, Lazarettstrasse, 36, 80636 Munich, Germany.
E-mail: joner@dhm.mhn.de

SUBMITTED ON 17/04/2017 - REVISION RECEIVED ON 1st 01/09/2017 / 2nd 05/11/2017 - ACCEPTED ON 16/11/2017

DOI: 10.4244/EIJ-D-17-00353

the heart including epicardial vessels and stents was transferred for detailed histopathologic assessment. Sections were prepared using the TissueSurgeon technology (LLS ROWIAK LaserLabSolutions GmbH, Hanover, Germany).

COMPUTATIONAL FLOW MODELLING

An OCT pullback from the six-month follow-up was used to create the geometry needed for simulation. Two longitudinal slices at right angles were obtained and the lumen of the artery was segmented from each slice. The segmented lumens were subsequently meshed and flow simulations were performed using ANSYS Fluent (ANSYS, Inc., Canonsburg, PA, USA). Blood was simulated as a Newtonian fluid with a density of 1,060 kg/m^3 and a viscosity of 0.0035 Pa.S. A boundary condition of a parabolic flow with a peak velocity of 0.5 m/s was imposed on the inlet of the vessel. Shear rate contours, wall shear stress of the vessel walls as well as velocity streamlines were obtained from the simulation results and superimposed on the original longitudinal OCT slices.

Results

At baseline, OCT showed well-apposed scaffold struts of the Absorb BVS with substantial underlying restenosis (layered pattern by OCT) of the metallic stent, and mild underexpansion of the proximal stented segment **(Moving image 3)**. At six-month angiographic follow-up, OCT revealed moderate tissue ingrowth between and above stent struts, with peri-strut thrombus formation within the proximal stented segment and attenuated plaque within the proximal transition zone from stented to non-stented vascular segments **(Moving image 4)**. At the time point of ST, OCT revealed massive remaining thrombus burden following thrombus aspiration and disrupted fibrous cap within the proximal transition zone **(Moving image 5)**. Culprit lesion morphology at the time point of scaffold thrombosis revealed acute plaque rupture within the transition zone from proximal non-stented to stented vascular segments; interestingly, co-registered frames from OCT pullbacks at baseline (index stenting) and six-month follow-up revealed fibrocalcific plaque without disrupted fibrous cap and fibrocalcific plaque with presumably disrupted fibrous cap (mean cap thickness 138±12 µm) and attenuation, respectively **(Supplementary Figure 1)**.

Results of histopathological assessment, OCT evaluation and computational flow modelling are presented in **Figure 1-Figure 3**.

Discussion

The main lessons to be learned from the current case can be described as follows:

(i) The cause of scaffold thrombosis was acute plaque rupture within the transition zone from proximal stented to non-stented vascular segments of the LAD. Significant underexpansion of the proximal scaffold portion was observed between baseline (index stenting) and six-month follow-up, which resulted in high shear stress and disturbed laminar flow and probably triggered plaque rupture just proximal to the scaffold **(Supplementary Figure 2A-Supplementary Figure 2C)**.

(ii) The Absorb BVS showed advanced vascular healing in the distal scaffold portion. Sections located more centrally revealed substantial heterogeneity in vascular healing with largely uncovered stent struts, fibrin deposition and acute inflammatory response.

(iii) Computational flow modelling of OCT imaging at six-month follow-up revealed increased shear stress in the region where plaque rupture occurred at 13 months following Absorb BVS implantation and maximum recirculation zones within and distal to the region of plaque rupture, which probably resulted in thrombus formation along the scaffolded vascular segment. Furthermore, it may be speculated that high shear stress arising from incompletely apposed and bulky stent struts within the proximal transition zone may also have contributed to the development of plaque rupture.

Conclusion

The current case report sheds further light on late events occurring following Absorb BVS implantation by combining detailed intravascular imaging with histopathological assessment of post-mortem coronary arteries. Dedicated studies investigating the Absorb BVS in the setting of in-stent restenosis remain highly limited, and the current case demonstrates that vascular healing is likely to be delayed in the setting of in-stent restenosis, where uncovered and malapposed stent struts with irregular surface lining are observed six months following scaffold implantation and persist up to 13 months. Consequently, increased shear stress and recirculation zones within proximal stented sections arising from malapposed and uncovered stent struts probably facilitated rupture of a thin fibrous cap, which manifested in very late scaffold thrombosis (VLST).

Impact on daily practice

The current case report demonstrates that progression of atherosclerosis may be an important determinant of very late scaffold thrombosis, where multiple risk factors may interact. Covering the entire lesion from healthy to healthy vascular segments may be critical to avoid late adverse events.

Funding

The research leading to these results has received funding from the European Union Seventh Framework Programme FP7/2007-2013 under grant agreement number HEALTH-F2-2010-260309 (PRESTIGE).

Conflict of interest statement

The authors have no conflicts of interest to declare.

References

1. Prati F, Guagliumi G, Mintz GS, Costa M, Regar E, Akasaka T, Barlis P, Tearney GJ, Jang IK, Arbustini E, Bezerra HG, Ozaki Y,

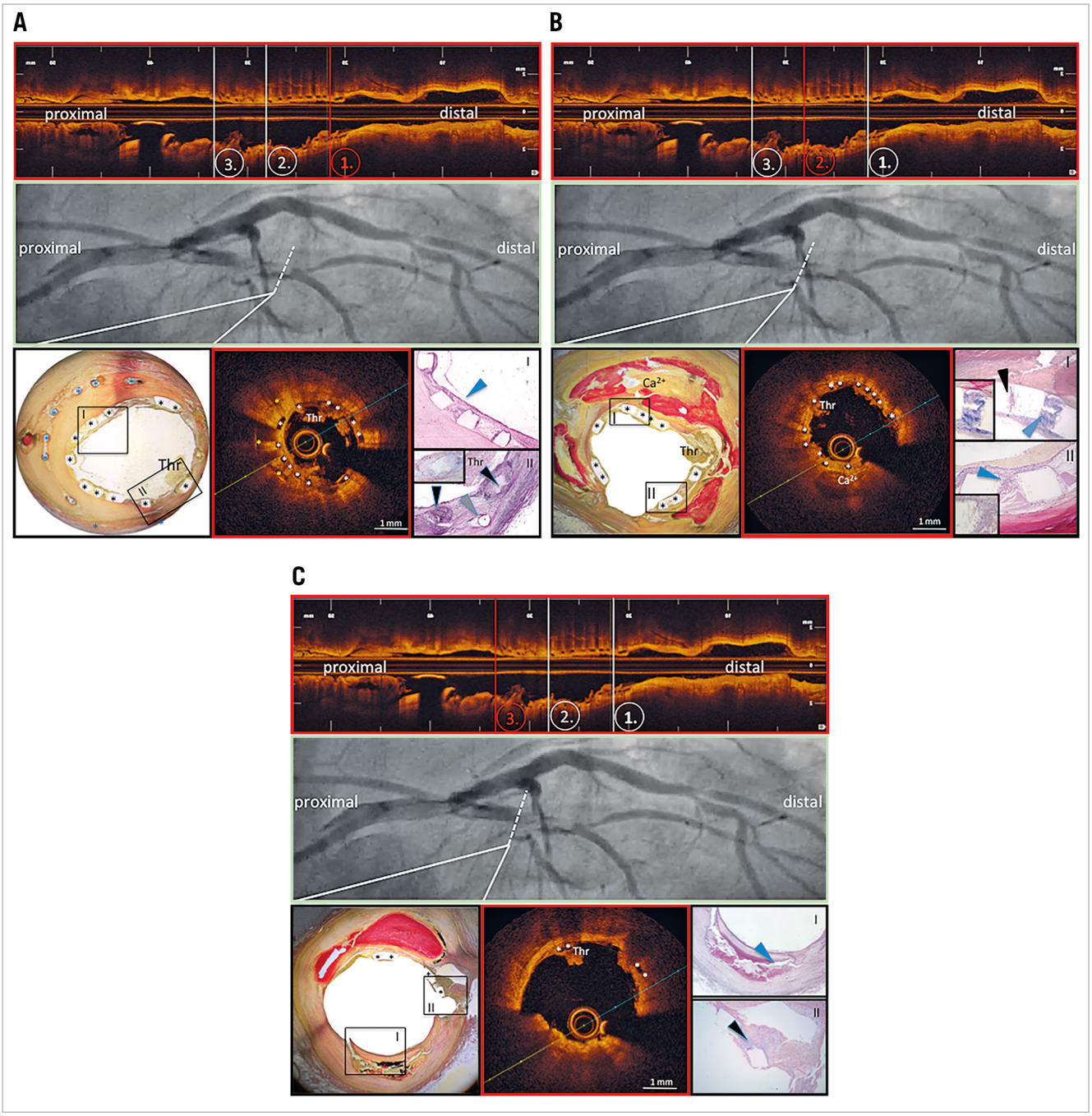

Figure 1. *Co-registered angiographic views, OCT frames and histopathological cross-sections. A) Distal scaffold segment. B) Middle scaffold segment. C) Proximal scaffold segment. Stent struts are depicted by asterisks (*); the blue arrowhead in panel A (I) points to a thin neointimal layer with good incorporation of scaffold struts into neointimal tissue; black arrowheads in panel A (II) point to inflammatory reactions in the surrounding of scaffold struts, with predominance of giant cell reactions (insert); grey arrowhead points to metallic stent strut. The cross-sectional OCT frame reveals overlapping stent struts, with translucent bioresorbable scaffold struts (white asterisks) on top of metallic stent struts (yellow asterisks). There is circumferential thrombus formation (Thr) limiting light penetration into the deeper neointimal regions. Black arrowhead in panel B (I) points to signs of scaffold strut degradation, with absorption of basic stain into the polymeric strut structure, while blue arrowheads (I & II) point to acute peri-strut inflammatory reactions (note the presence of fibrin staining in dark blue). The cross-sectional OCT frame reveals significant thrombus formation on top of translucent scaffold struts (white asterisks), with presence of calcification behind stent struts at 6 o'clock (Ca2+). The blue arrowhead in panel C (I) points to the large necrotic core underlying rupture of a thin fibrous cap; the black arrowhead (II) points to thrombus formation in the setting of scaffold struts obscuring a side branch. The cross-sectional OCT frame shows the presence of irregular, attenuating tissue prolapsing into the lumen, highly suggestive of acute plaque rupture with superficial thrombus formation at 6 o'clock, while there is thrombus adhering to scaffold struts (white asterisks) at 11 o'clock (Thr). Thr: thrombus*

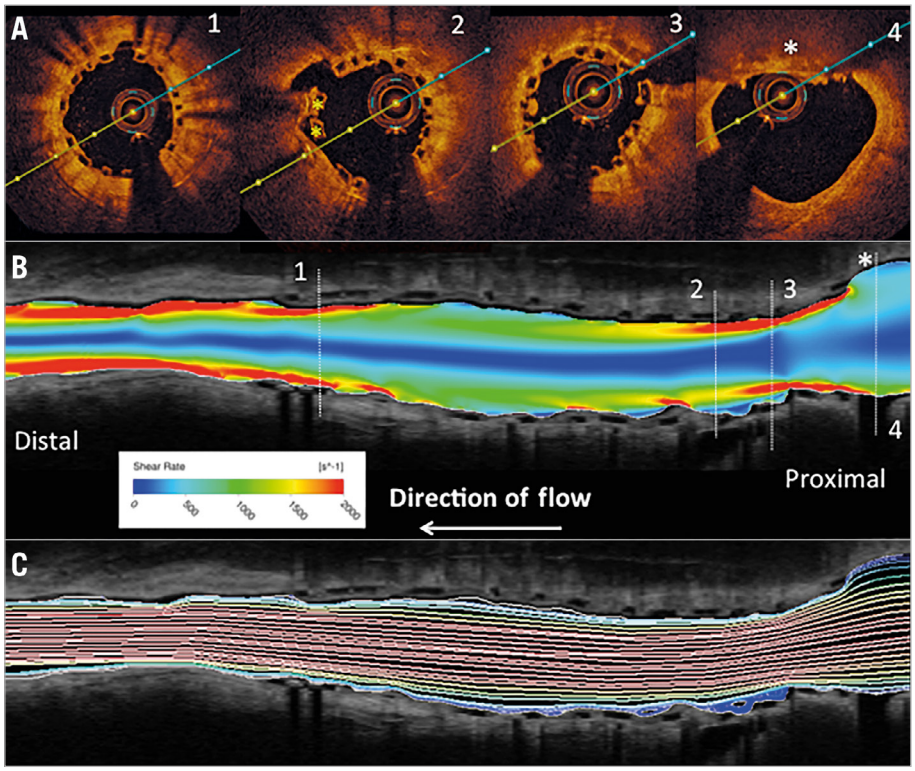

Figure 2. *Co-registration of cross-sectional (A) with longitudinal OCT frames (B & C) including computational flow modelling of shear rate and recirculation zones. Note, there is increased shear rate observed in the transition zone from proximal non-stented to stented vascular segments (red colour in B) and within the middle to distal underexpanded stented segments. Mild recirculation zones are observed distal to the presumed rupture site (blue colour in C).*

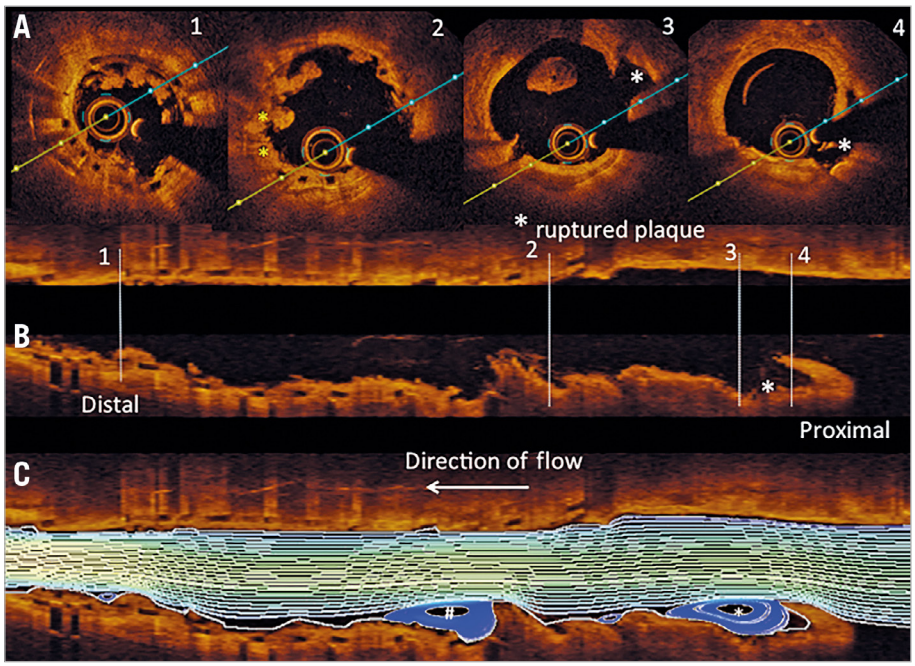

Figure 3. *Co-registration of cross-sectional (A) with longitudinal OCT frames (B & C) including computational flow modelling of recirculation zones. Note, there are excessive recirculation zones observed distal to the site of plaque rupture (white asterisk), which probably contributed to thrombus formation along the proximal scaffolded segment. Another area of excessive recirculation zones is observed further distal in the scaffolded vascular segment, which is probably the result of protruding thrombus (white hash key).*

Bruining N, Dudek D, Radu M, Erglis A, Motreff P, Alfonso F, Toutouzas K, Gonzalo N, Tamburino C, Adriaenssens T, Pinto F, Serruys PW, Di Mario C; Expert's OCT Review Document. Expert review document part 2: methodology, terminology and clinical applications of optical coherence tomography for the assessment of interventional procedures. *Eur Heart J.* 2012;33:2513-20.

2. Tearney GJ, Regar E, Akasaka T, Adriaenssens T, Barlis P, Bezerra HG, Bouma B, Bruining N, Cho JM, Chowdhary S, Costa MA, de Silva R, Dijkstra J, Di Mario C, Dudek D, Falk E, Feldman MD, Fitzgerald P, Garcia-Garcia HM, Gonzalo N, Granada JF, Guagliumi G, Holm NR, Honda Y, Ikeno F, Kawasaki M, Kochman J, Koltowski L, Kubo T, Kume T, Kyono H, Lam CC, Lamouche G, Lee DP, Leon MB, Maehara A, Manfrini O, Mintz GS, Mizuno K, Morel MA, Nadkarni S, Okura H, Otake H, Pietrasik A, Prati F, Raber L, Radu MD, Rieber J, Riga M, Rollins A, Rosenberg M, Sirbu V, Serruys PW, Shimada K, Shinke T, Shite J, Siegel E, Sonoda S, Suter M, Takarada S, Tanaka A, Terashima M, Thim T, Uemura S, Ughi GJ, van Beusekom HM, van der Steen AF, van Es GA, van Soest G, Virmani R, Waxman S, Weissman NJ, Weisz G; and International Working Group for Intravascular Optical Coherence Tomography (IWG-IVOCT). Consensus standards for acquisition, measurement, and reporting of intravascular optical coherence tomography studies: a report from the International Working Group for Intravascular Optical Coherence Tomography Standardization and Validation. *J Am Coll Cardiol.* 2012;59:1058-72.

Supplementary data

Supplementary Figure 1. Co-registration of cross-sectional OCT frames from baseline, six-month follow-up and the time point of scaffold thrombosis.

Supplementary Figure 2. OCT core laboratory measurements for the entire scaffolded segment at baseline, six-month follow-up and the time point of scaffold thrombosis.

Moving image 1. Good angiographic result at follow-up after BVS implantation.

Moving image 2. TIMI 2 flow in the LAD during PTCA for STEMI.

Moving image 3. OCT pullback in the LAD after BVS implantation ("baseline") with well-apposed scaffold struts and mild underexpansion.

Moving image 4. OCT pullback in the LAD at follow-up after six-month OCT with moderate tissue ingrowth between and above stent struts, peri-strut thrombus formation within the proximal stented segment and attenuated plaque within the proximal transition zone from stented to non-stented vascular segments.

Moving image 5. OCT pullback in the LAD at STEMI, revealing massive thrombus burden following thrombus aspiration and disrupted fibrous cap within the proximal transition zone.

The supplementary data are published online at: http://www.pcronline.com/eurointervention/133rd_issue/358

Supplementary data

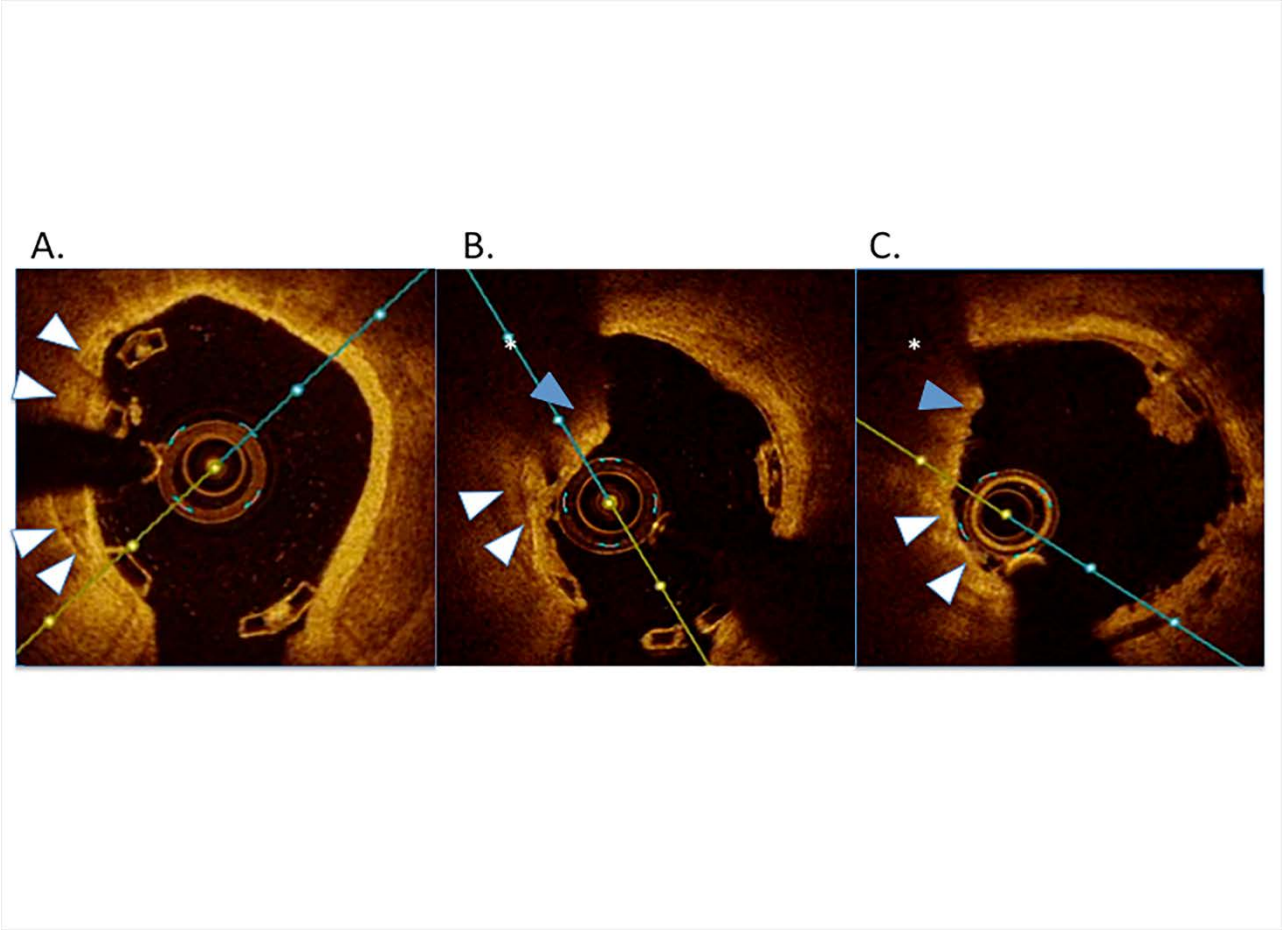

Supplementary Figure 1. Co-registration of cross-sectional OCT frames from baseline, six-month follow-up and the time point of scaffold thrombosis.

A) From baseline (index stenting); B) six-month follow-up; and C) time point of scaffold thrombosis.

Note, there is underlying fibrocalcific plaque (A, white arrowheads) with intact fibrous cap, which progressed into fibrocalcific plaque with presumably disrupted fibrous cap and attenuation (B, blue arrowhead) at six-month follow-up, and further into plaque rupture of a thin-cap fibroatheroma (C, blue arrowhead) at the time point of scaffold thrombosis (13 months after index stenting).

A.

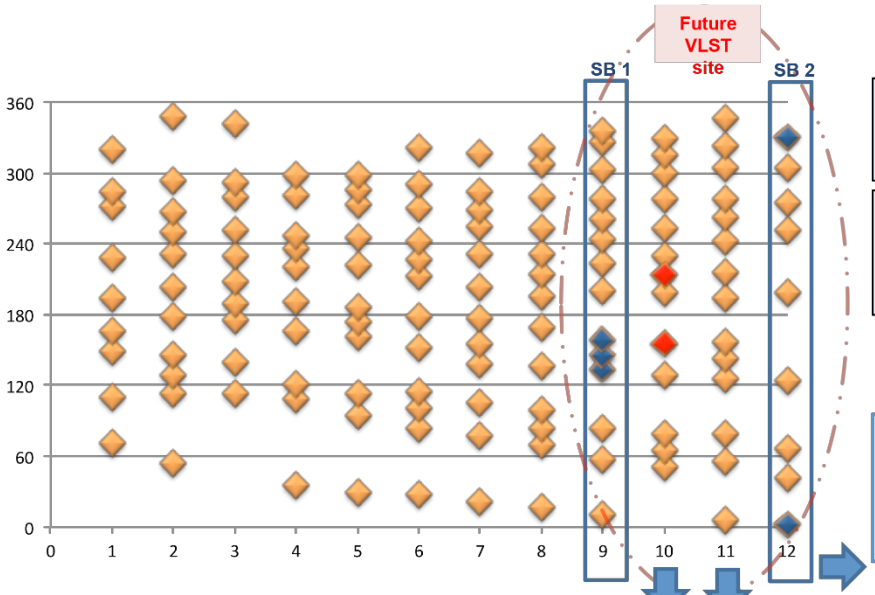

Stented seg. length= 11.5 mm
Visible struts= 138
Uncovered struts= 136 (98.55 %)
Malapposed struts= 2 (1.45 %)

Avg. lumen area= 4.86 mm^2
Min. lumen area= 3.23 mm^2

Avg. stent area= 4.37 mm^2
Min. stent area= 2.92 mm^2

Frame 12:
(A) Stent area= 3.70 mm^2;
(B) Minimum lumen area
(Proximal ref. segment): 5.73 mm^2

Stent Expansion= 64.57%

Frame 10:
(A) Stent area= 3.65 mm^2;
(B) Minimum lumen area
(Proximal ref. segment): 5.73 mm^2

Stent Expansion= 63.70%

Frame 11:
(A) Stent area= 2.92 mm^2;
(B) Minimum lumen area
(Proximal ref. segment): 5.73 mm^2

Stent Expansion= 50.96%

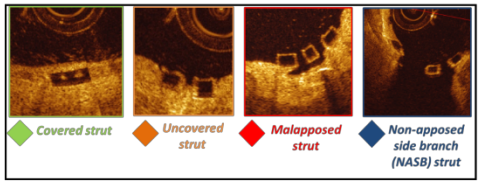

B.

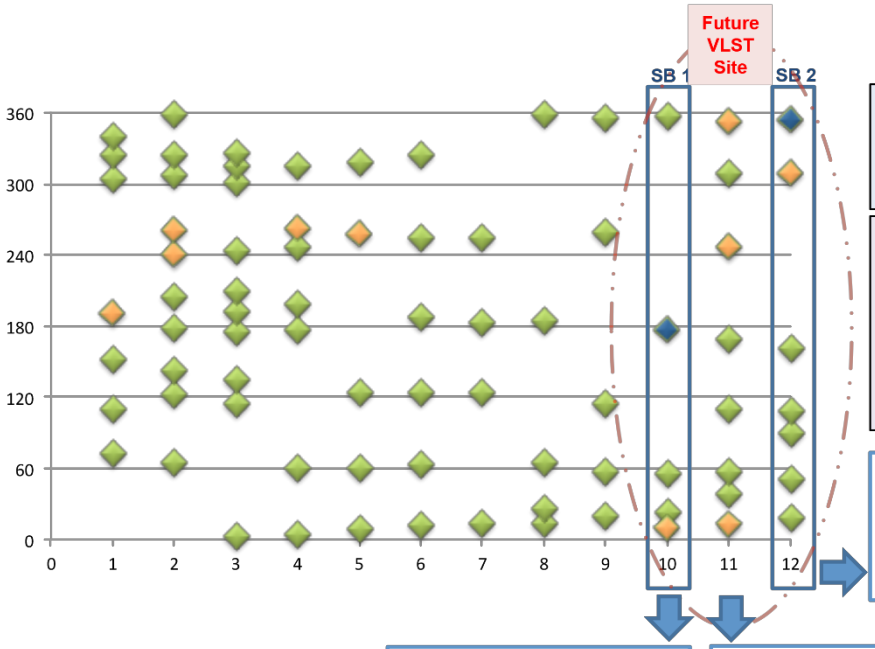

Stented seg. length= 11.7 mm
Visible struts= 79
Covered struts= 67 (84.81 %)
Uncovered struts= 10 (12.66 %)
Malapposed struts= 0 (0.0 %)

Avg. lumen area= 3.95 mm²
Min. lumen area= 2.87 mm²

Avg. stent area= 4.04 mm²
Min. stent area= 2.73 mm²

Mean neointimal area= 0.13 mm²
Min. neointimal area= -0.16 mm²
Mean % area stenosis= 2.23 %

Frame 12:
(A) Stent area= 3.70 mm²;
(B) Minimum lumen area
(Proximal ref. segment): 4.97 mm²

Stent Expansion= 74.44%

Frame 10:
(A) Stent area= 4.25 mm²;
(B) Minimum lumen area
(Proximal ref. segment): 4.97 mm²

Stent Expansion= 85.51%

Frame 11:
(A) Stent area= 2.73 mm²;
(B) Minimum lumen area
(Proximal ref. segment): 4.97 mm²

Stent Expansion= 54.93%

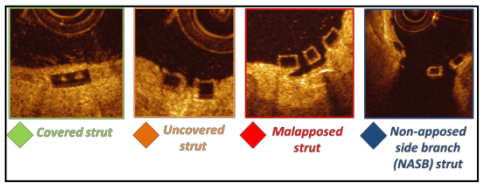

C.

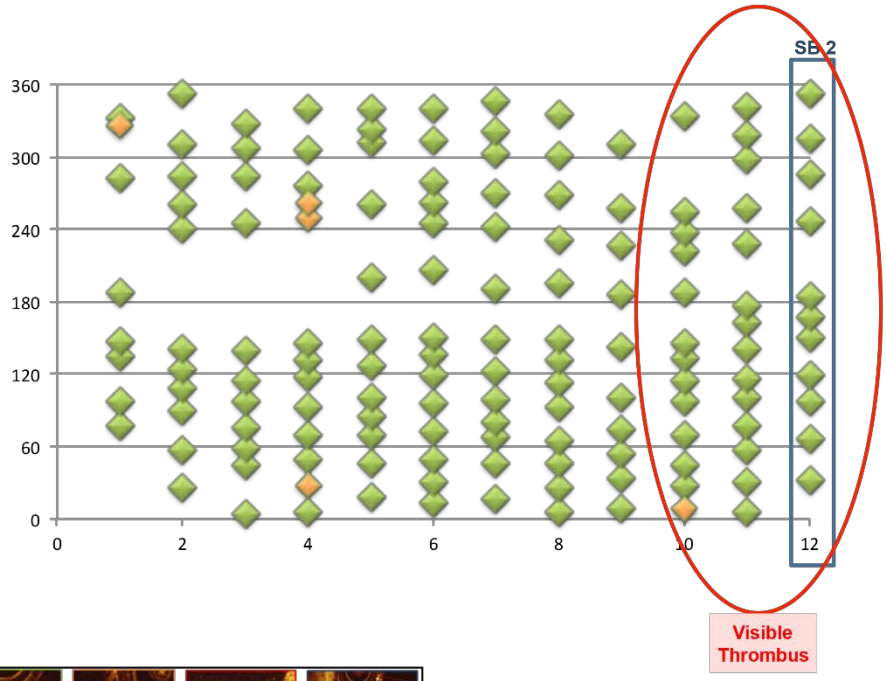

Stented seg. length= 11.3 mm
Visible struts= 118
Covered struts= 113 (95.76 %)
Uncovered struts= 5 (4.24 %)
Malapposed struts= 0 (0.0 %)

Avg. lumen area= 3.71 mm²
Min. lumen area= 2.80 mm²

Avg. stent area= 4.13 mm²
Min. stent area= 2.80 mm²

Mean neointimal area= 0.58 mm²
Min. neointimal area= 0.31 mm²
Mean % area stenosis= 10.17 %

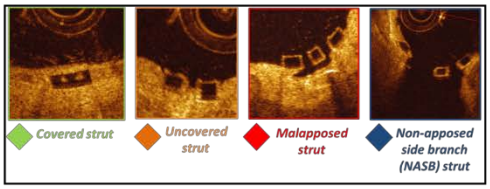

Supplementary Figure 2. OCT core laboratory measurements for the entire scaffolded segment at baseline, six-month follow-up and the time point of scaffold thrombosis.

OCT core laboratory measurements were performed using QIvus® software, Version 3.0.30.0 (Medis medical imaging systems, Leiden, the Netherlands) for the entire scaffold segment at baseline (index stenting, A), six-month follow-up (B) and at the time point of scaffold thrombosis (C). Stent area was assessed with the help of automatic strut contour detection, where a circular line was drawn by connecting endoluminal centre points of each translucent scaffold strut. Lumen area was traced by connecting the endoluminal surface of scaffold struts with the intimal surface between scaffold struts along the entire circumference of the scaffold cross-section. Neointimal area was calculated as: stent area – lumen area. Percent area stenosis was calculated as: (stent area–lumen area)/stent area*100. Uncovered stent struts were qualitatively assessed as uncovered with visible neointimal tissue. Malapposed stent struts were determined when there was a clearly visible gap between the intimal surface of the scaffold strut and the intima. Scaffold struts placed above side branches were not considered as uncovered or malapposed. Stent expansion was calculated as: (stent area in a particular frame/minimum lumen area in the reference segment nearest to that particular frame) x100. Reference segments were typically those within 10 mm of either edge of the stent (but within the same vessel segment).